Journal of Research in Pharmacy

Research Article

www.jrespharm.com

Intranasal delivery of levosulpiride-decorated novel nanosized phospholipid magnesomes for the treatment of schizophrenia: Development, optimization, and *in vitro* characterization

Ravish J. PATEL [1] *, Nidhi TRIVEDI [1], Vidhi PANDYA [1], Amit A. PATEL [1], Samir G. PATEL [1], Bhupendra G. PRAJAPATI [2]

[1] Department of Pharmaceutics and Pharmaceutical Technology, Ramanbhai Patel College of Pharmacy, Charotar University of Science and Technology, Changa- 388421, Anand, Gujarat, India.

[2] Department of Pharmaceutics and Pharmaceutical Technology, S.K. Patel College of Pharmaceutical Education & Research, Ganpat University, Ganpat Vidyanagar- 384012, Mehsana, Gujarat, India.

* Corresponding Author. E-mail: ravishpatel.ph@charusat.ac.in (R.J.P.); Tel. +91-992-465 92 16.

Received: 27 May 2023 / Revised: 18 January 2024 / Accepted: 20 January 2024

ABSTRACT: Levosulpiride (LSP) has been studied for its wide medicinal potential. One of its uses is in the treatment of schizophrenia. LSP has limited oral bioavailability because of its low permeability, dissolvability, and P-Glycoprotein (P-gp) efflux effect. Contrary to conventional methods, the intranasal route provides safe and effective treatment as well as targeted action. It can also prevent the P-gp efflux effect and increase brain bioavailability. In this research, we aimed to develop LSP-loaded Phospholipid Magnesomes (PMs), a novel vesicular nanosystem, recently fabricated for brain targeting by the Ultra-sonication method with materials including Phospholipon 90G, the combination of Propylene glycol and ethanol, magnesium sulphate (MgSO4) and water. The Box-Behnken design was utilized with 29 runs to optimize the LSP-PMs formulation. The formulation was confirmed and evaluated by the FTIR, DSC, PXRD, and TEM study. The formulation was investigated in vitro at pH 6.4, and the results showed that the formulation had improved drug release. The optimized LSP-PMs formula had a vesicle sizing of 85.035 ± 2.77 nm, a PDI of 0.392 ± 0.69, and a %EE of 76.024 %. Spherical and multilamellar morphology of LSP-PMs were visible by the TEM. The optimized LSP-PMs had the quickest medication diffusing profile, achieving 100% in one hour. The LSP-PMs formulation was stable at room temperature for 50 days when screened for the stability study. Thus, to sum up, the nano-vesicular system of LSP-PMs demonstrated to be a promising formulation for enhancing drug release of the poorly water-soluble and permeable LSP. Further investigation to analyze nasal transport to the brain, pharmacokinetic and pharmacodynamic effects, local safety, and the behavior of the developed carrier will require additional research.

KEYWORDS: Levosulpiride; schizophrenia; phospholipid magnesomes; antipsychotic drug; intranasal drug delivery systems; brain targeting; box-behnken design

1. INTRODUCTION

Schizophrenia is a persistent psychotic condition that interferes with the victim's ideas and emotions [1]. There are three categories of schizophrenia symptoms: cognitive, negative, and positive. Positive symptoms comprise abnormal behaviors and thoughts, such as recurring psychosis, defined as a "loss of contact with reality" characterized by delusions, disorganization of behavior, speech, and hallucinations. Negative symptoms of the amotivational syndrome include social withdrawal, affective flatness, anhedonia (the inability to perceive pleasure), and decreased initiative and energy. Lastly, cognitive symptoms are manifested as a diverse variety of cognitive dysfunctions, including executive function, working memory, and processing speed deficiencies [2,3].

Neurotransmission abnormalities have been used to support theories about the pathogenesis of schizophrenia. Almost all of these hypothesis center on either surplus or lack of neurotransmitters like serotonin, dopamine, and glutamate. Different studies connect aspartate, glycine, and gamma-aminobutyric acid (GABA) to the neurochemical imbalance of schizophrenia [4]. Many schizophrenia symptoms are thought to be linked to aberrant dopamine receptor activity (particularly D2).

How to cite this article: Patel R, Trivedi N, Pandya V, Patel A, Patel S, Prajapati B. Intranasal delivery of levosulpiride-decorated novel nanosized phospholipid magnesomes for the treatment of schizophrenia: Development, optimization, and invitro characterization. J Res Pharm. 2024; 28(5): 1674-1690.

ISSN: 2630-6344

http://dx.doi.org/10.29228/jrp.843

Levosulpiride (LSP) is the hydrophobic enantiomer of sulpiride (levorotatory), a commuted benzamide with a long history of therapeutic usage in Europe and around the world. It is extensively utilized as an antipsychotic, antiulcer, antiemetic, and antidyspeptic, which addresses somatoform disorders, psychosis, emesis, dyspepsia, and melancholy. It inhibits dopaminergic receptors (D2) in the Central Nervous System (CNS) and the gastrointestinal pathway [5,6]. It has been identified as a BCS class IV compound and a P- tract, glycoprotein substrate (P-gp) [7]. As a result of its sparing water solubility, restricted absorption in the gastrointestinal and effect of P-glycoprotein efflux, LSP has modest oral absorption (20–30%) [8].

LSP is typically delivered orally and intravenously and is available commercially as a regular-release tablet, capsule, and injection. The recommended starting dose for LSP is 25 mg, 20 mg, and 12.5 mg for tablets, capsules, and injections, respectively. However, the low bioavailability due to low gastrointestinal absorption, low water solubility, P-glycoprotein efflux, and also problematic side effects due to high doses, like a disturbance in sleep, agitation, overstimulation, and mild extrapyramidal and cardiovascular effects, makes the standard LSP oral and intravenous drug delivery unfavourable [9,10]. Furthermore, Active Pharmaceutical Ingredient (API) distribution to the CNS endure a significant problem for medications affecting CNS; greater than 98% of small-molecule pharmaceuticals are unable to penetrate the CNS from the circulation, and the percentage rises to almost 100% for bigger-molecule pharmaceuticals [11]. It could be owing to the Blood Brain Barrier's (BBB) presence, that prohibits practically all medication molecules, numerous phytoconstituents, proteins, peptides, and other big compounds from entering the brain in order to protect it from damage [12,13]. This all contributes to searching for another pathway that administers the medication directly to the CNS [12].

The Intranasal (IN) route stands out as a pleasant and efficient method which avoids the BBB and delivers the active molecule straight to the brain via the nasal passage [12]. Because of the unique relationship between the nose and the CNS, medicinal drugs can be administrated to the brain via the route of intranasal [14]. The nasal approach skips the BBB and prevents the P-glycoprotein efflux system.

The olfactory and trigeminal neural pathways provide a direct connection to transfer therapeutically active molecules to the brain. Initially, direct delivery was attributed to the olfactory route [15]. The main advantage of IN route is that it provides non-invasive administration for local or systemic effects in IN administration, discovered to be a quick, safe, cost-effective and satisfying alternative to parenteral drug administration. Furthermore, it is a handy and simple method for administering a drug in emergencies that do not necessitate professional medical personnel or hospitalization [16–19].

Nanotechnology is actively used in Intranasal drug delivery technology for directly targeting the active molecules in the brain [19]. In contrast, the delivery of hydrophilic compounds, peptides, and proteins to the brain is poor when employing traditional nanocarriers [20]. Thus, the new nanocarrier has been investigated for IN delivery, enhancing drug delivery to the brain. This nanocarrier is known as Phospholipid Magnesomes (PMs), which was designed by Natsheh and Touitou [21]. It is utilized to transport peptides, proteins, and tiny compounds to the brain. PMs comprise soft phospholipid vesicles, water (buffer), and magnesium salt [20,22]. Ethanol-containing PMs could improve vesicular system permeability and penetration while stabilizing PM [22–24]. PMs are the modified version of the Liposomes, which are altered to improve brain bioavailability. Studies have shown that PMs improve therapeutic drug administration through the nasal route to the brain by allowing for both extracellular and intracellular transit of Active Pharmaceutical Ingredients (API) to the CNS [22].

Thus, this study intended to develop and assess PMs to enhance the delivery of a LSP to the brain through intranasal administration. Phospholipid and $MgSO_4$ were used to enhance the drug's permeation through the nasal mucosa and increase its effectiveness. Box-Behnken design (BBD) was utilised by the Design Expert (DoE, version 13, State-Ease Inc., Minneapolis, USA) programme to optimise PMs produced by the sonication process. The LSP-PMs were analyzed to ascertain their physicochemical properties. The optimized formulation was subsequently evaluated for *invitro* drug release.

2. RESULTS and DISCUSSION

2.1. Optimization by Box-Behnken Designs

The ultrasonication approach was applied to create 29 LSP formulations based upon BBD. The BBD was selected due to its appropriateness, for instance comprising less than 6 factors and 3 levels. The approach encounters several benefits such as fewer experiments in comparison to the central composite

design (CCD), accommodates non-linear impacts, and is suitable for optimizing both products and processes. The constraints of CCD, such as its 5-level constraint and the requirement for an extensive number of experiments, led to the selection of BBD as the optimal design above other options for the optimization of the formulation. Table 1 depicts the recorded values of the three responses, namely vesicle size, PDI, and percent entrapment efficiency, for all batches. The three measured responses were found to be influenced by the independent factors chosen. All batches had vesicle sizes ranging from 85.0367 ± 1.304 to 337.9 ± 15.933 nm, PDI ranging from 0.227 ± 0.002 to 0.513 ± 0.011, and EE% ranging from 40.946 to 86.736%. Because formulation features (responses) are highly dependent on their values and levels, substantial shifts in retaliation data when the variable or/and its level change suggest an independent factor selection adequacy. The polynomial equations containing the primary impacts and interacting factors were computed using the software's ANOVA provision based on the assessment of different statistical parameters [25,26].

These findings corroborated the calculated acceptable precision ratios and demonstrated the significance of the equations of the model recommended for navigating the design space. Contour plots were created for additional exploration of the impact of a few independent factors on the intended outcome, where at a fixed level of the third component, factorial interactive binary effects on definite responses can be investigated. Plots were made to monitor any response's performance when only one element varied within the planned restriction range while the other two remained fixed. Additionally, they make it possible to compare every aspect at any stage of the design space.

2.1.1. Independent variables outcome on Vesicle size

Colloidal lipoid system vesicle size is a challenging procedure since it is regulated by the variety of lipids and solvents employed, their quantities, and their relative percentage. It can also be adjusted by the formulating parameters of sonication and/or homogenization time and speed [26,27]. The PS ranged from 85.0367 ± 1.304 to 337.9 ± 15.933 nm, according to the values shown in Table 1 and depicted in Figure 1. The polynomial regression equations below for the linear model quantified the result of A, B, C, and D on VS:

Vesicle size = + 128.17 + 10.61 A (p=0.0361) – 11.65 B (p=0.0426) – 21.62 C (p=0.0271) – 30.76 D (p=0.0191) – 3.59 AB (p=0.0043) – 2.34 AC (p=0.0111) – 2.32 AD (p=0.0120) + 9.28 BC (p=0.0491) +15.32 BD (p=0.0468) + 56.71 CD (p=0.0135) (R^2=0.9257)

Vesicle size can be predicted using this coding equation at a different level of the given independent component. A + value of a factor coefficient represents a proportional impact on the result, and a - value represents an inverse relation among the tested response and this factor.

As per figure 1, model terms C along with D have a notable effect upon the VS of the prepared LSP-PMs system. The antagonistic impact on vesicle size is demonstrated by the negative sign of the coefficients for both variables. The results depicted that by increasing the quantity of Propylene glycol (C) and the time of sonication (D), there was a reduced size of the vesicle.

Also, by increasing the amount of ethanol (B), there was a decrease in vesicle size. In systems containing lipids, raising the lipid amount causes the development of bigger vesicles because of the increased propensity of lipids which can coalesce with the increasing amount, resulting in greater viscosity and uniformity of the formulation and a rise in surface tension [26,28]. So, because of this, it was seen that by increasing the amount of lipid (A), there was an agonist effect as it increased the size of the vesicle.

2.1.2. Independent variables outcome on PDI

The PDI is a criterion that states the homogeneity of the VS distribution. The range spans from 0.0 to 1.0. The PDI outcome becomes more indicative of particle homogeneity as it gets closer to zero [29]. It is computed using the measured mean particle size and standard deviation of the specified dispersed system. Small PDI values indicate a restricted PS range of distribution with improved stability in homogenous, monodispersed systems [26,30]. The data in Table 1 and Figure 2 reveal that all manufactured batches of LSP-PMs had PDI values ranging from 0.26 ± 0.025 to 0.513 ± 0.011, showing that the prepared PMs systems had a reasonable size distribution and homogeneity. The below given polynomial regression equations for the linear model quantified the effect of A, B, C and D on PDI:

PDI = + 0.3899 + 0.0467 A (p=0.0032) – 0.0323 B (p=0.0302) – 0.0611 C (p=0.0003) – 0.0133 D (p=0.0468) – 0.0303 AB (p=0.0179) – 0.0132 AC (p=0.0262) – 0.0163 AD (p=0.0405) – 0.0175 BC (p=0.0408) – 0.0107 BD (p=0.0368) – 0.0462 CD (p=0.0473) (R^2=0.9135)

Table 1. LSP-PMs formulation composition and responses observed

	Independent Variables				Dependent Variables		
Run	A: Amount Of PL 90G	B: Amount of ethanol	C: Amount of PG	D: Sonication Time	Vesicle Size (mean ± SD)	PDI (mean ± SD)	EE
	gm	ml	ml	Min	nm		%
1	1.5	1	6	15	158.967 ± 2.779	0.461 ± 0.03	59.1
2	1.5	3	6	9	140.6 ± 1.992	0.424 ± 0.021	53.946
3	1	3	6	15	95.9433 ± 1.228	0.336 ± 0.032	44.736
4	2	5	6	9	108.733 ± 0.251	0.390± 0.002	57.526
5	1.5	3	3	3	337.9 ± 15.933	0.358 ± 0.041	61.73
6	1.5	3	3	15	100.01 ± 1.915	0.436 ± 0.016	72.262
7	1.5	3	6	9	132.7 ± 2.424	0.503 ± 0.088	59.89
8	1.5	3	6	9	142.9 ± 40.308	0.448 ± 0.005	65.946
9	1	3	9	9	105.333 ± 2.775	0.302 ± 0.028	40.946
10	1.5	1	9	9	102.567 ± 1.357	0.331 ± 0.015	62
11	2	3	6	3	164.533 ± 6.416	0.469 ± 0.014	80.156
12	1.5	3	6	9	111.933 ± 2.569	0.406 ± 0.012	68.578
13	2	3	6	15	126.333 ±1.721	0.392 ± 0.032	68.842
14	1	1	6	9	85.0367 ± 1.304	0.287 ±0.009	39.104
15	1	5	6	9	111.167 ±2.569	0.359 ± 0.008	42.788
16	1.5	5	6	15	111.833 ± 1.625	0.322 ± 0.036	62
17	2	3	3	9	124.567 ± 2.177	0.513 ± 0.011	86.736
18	2	1	6	9	96.9567 ± 1.090	0.440 ±0.018	77.788
19	1.5	5	9	9	110.067 ± 4.301	0.26 ± 0.025	55.42
20	1.5	1	3	9	143.2 ± 1.473	0.484 ± 0.028	65.156
21	1.5	5	3	9	113.567 ± 3.655	0.432 ± 0.025	69.368
22	1.5	3	9	3	112.133 ± 2.030	0.333 ± 0.031	62
23	1.5	1	6	3	216.167 ± 5.316	0.460 ± 0.034	63.578
24	1.5	3	6	9	109.467 ± 1.616	0.4 ± 0.002	65.684
25	1	3	3	9	95.9633 ± 2.294	0.388 ± 0.039	64.368
26	1.5	3	9	15	101.07 ± 1.196	0.227 ± 0.002	50.946
27	1.5	5	6	3	107.733 ± 0.321	0.364 ± 0.014	65.94
28	2	3	9	9	124.567 ± 4.772	0.375 ± 0.052	70.68
29	1	3	6	3	124.867 ± 2.466	0.348 ± 0.052	42

Just model terms A, B, and C were significant. The lipid concentration (A) had an agonistic impact on PDI. In other terms, the PDI increased as lipid concentration was increased. In contrast, the amount of ethanol (B), propylene glycol (C), and sonication time (D) had an antagonistic impact on PDI. In other terms, it can be expressed as increasing the amount of ethanol, propylene glycol, and time of sonication; there was a decrease in PDI.

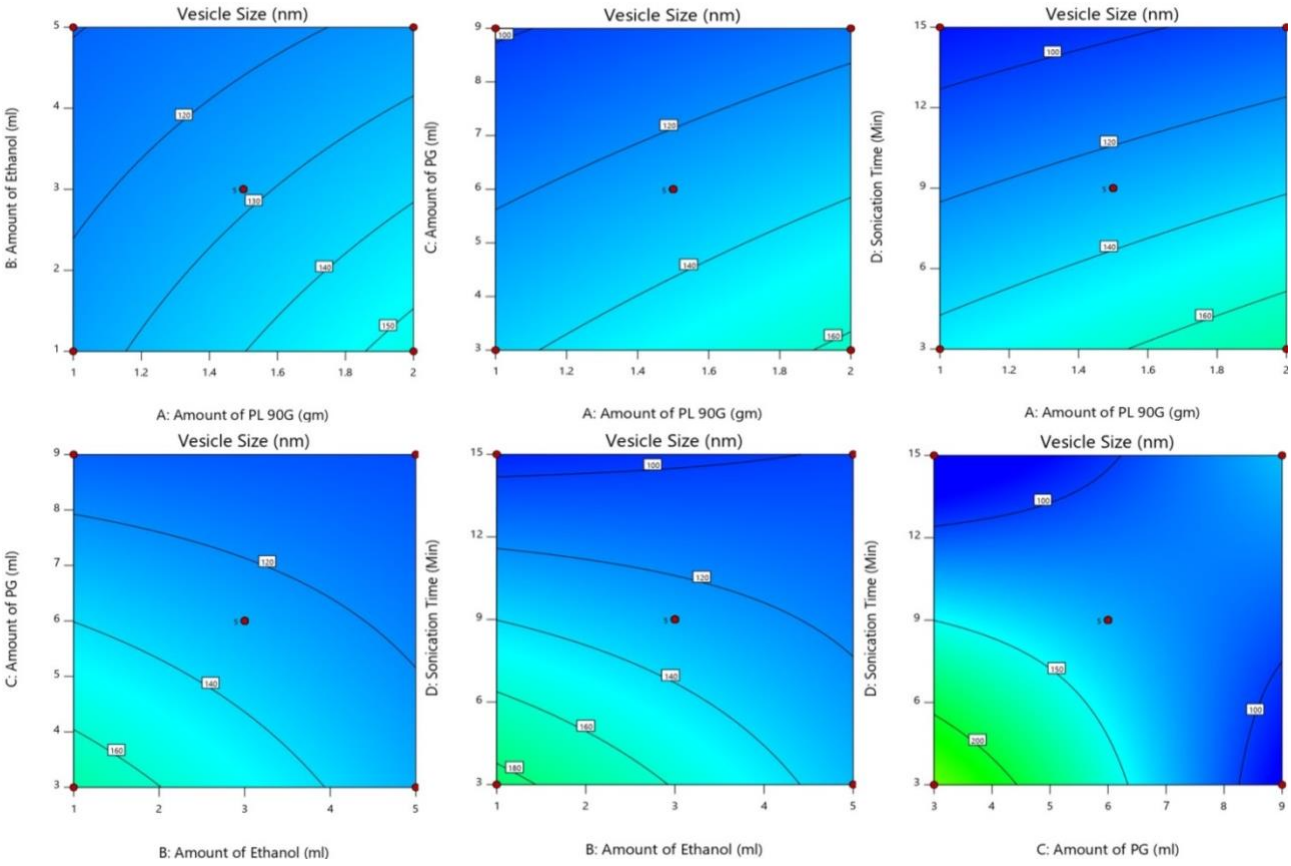

Figure 1. Contour plots depicting the effect of the amount of phospholipid (PL), ethanol, and propylene glycol (PG) and sonication time on the VS.

2.1.3. Independent variables outcome on %EE

The % EE was seen to be in the range of 40.946 to 86.736%, according to the values shown in Table 1 and represented in Figure 3. The polynomial regression equations for the linear model given below quantified the effect of A, B, C, and D on % EE.

% Entrapment efficiency = + 61.35 + 13.98 A (p=<0.0001) – 1.14 B (p=0.0105) – 6.47 C (p=0.0013) – 1.46 D (p=0.0011) – 5.99 AB (p=0.0468) + 1.84 AC (p=0.0392) – 3.51 AD (p=0.0479) – 2.70 BC (p=0.0312) + 0.1345 BD (p=0.0240) – 5.40 CD (p=0.0332) (R^2=0.9388)

As per the figure, model term A along with C had a notable result on % EE. The primary impacts of lipid percentage (A) on EE percentage were synergistic. In other words, as the quantity of lipids increased, so did the EE%. The content of propylene glycol (C) is the second important element influencing the EE%. It has an antagonistic effect on the formulation, i.e., when the concentration of propylene glycol is increased, the %EE is decreased.

2.1.4. Validation and optimization of the results obtained

Table 2 shows satisfactory accord among noted and expected numerical data for the three answers among the suggested restrictions of the evaluated factors, which are independent based on the recommended design matrix and computed desirability. All these findings support the chosen optimization strategy and the applicability of the resulting regression model equations for predicting VS, PDI, and EE percent of LSP-PMs at the examined formulation variable levels.

Based on the previous assessment data, the optimized LSP-PMs formula (F3) was developed and tested further for other parameters like TEM, XRD, DSC, *Invitro* studies. It consisted of 2 g of a phospholipid, 3.833 ml of ethanol, 8.997 ml of propylene glycol, and 3.527 minutes of sonication duration having vesicle size of 89.65 ± 1.721, 0.392 ± 0.002 PdI and 76.6% EE.

Journal of Research in Pharmacy
Research Article

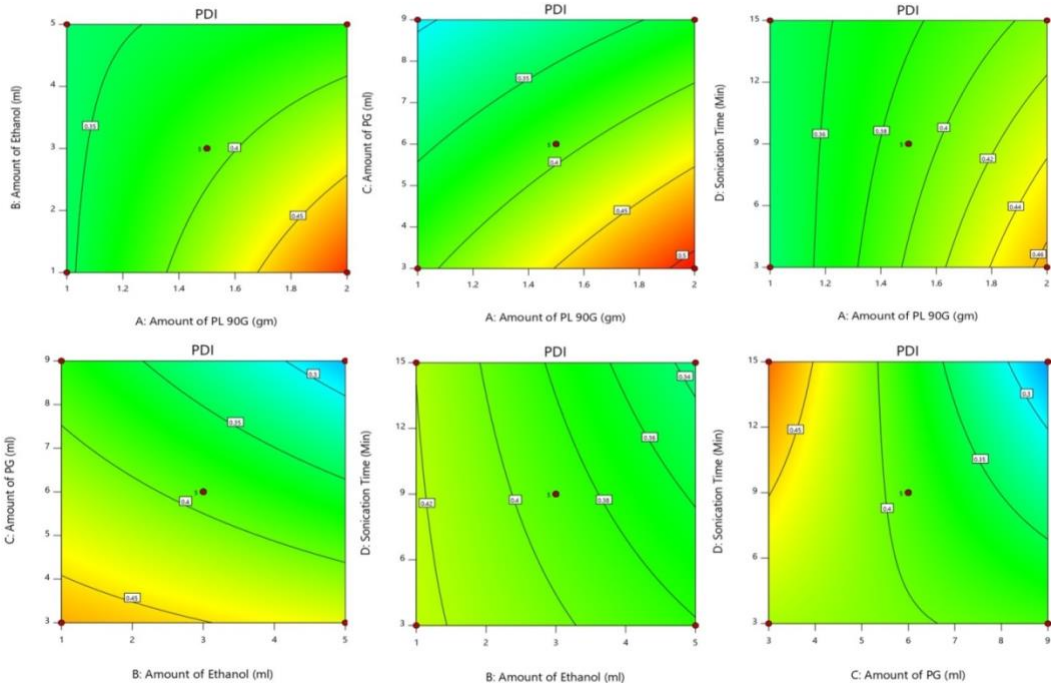

Figure 2. Contour plots depicting the effect of the amount of phospholipid (PL), ethanol, and propylene glycol (PG) and sonication time on PDI value.

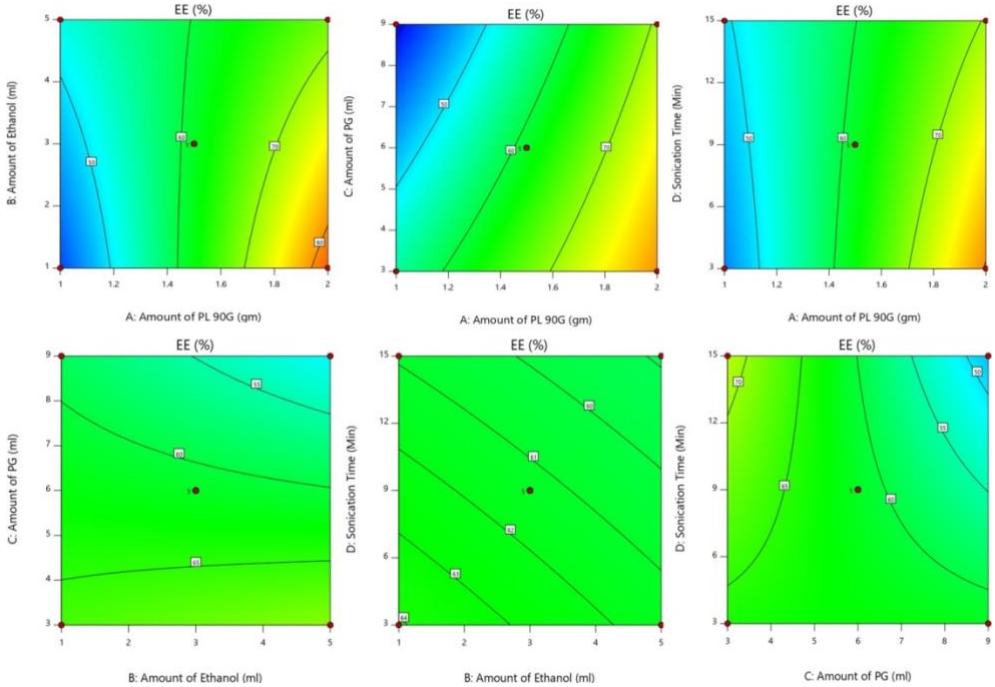

Figure 3. Contour plots depicting the effect of the amount of phospholipid (PL), ethanol, and propylene glycol (PG) and sonication time on the % EE.

http://dx.doi.org/10.29228/jrp.843
J Res Pharm 2024; 28(5): 1674-1690

Table 2. Formulation of the optimum LSP-PMs formulations chosen with varying expected and actual response values.

Formula	Composition				Response	Predicted	Observed	P Value	Desirability
	A	B	C	D					
F1	2.0 g	4.425 ml	9.0 ml	4.563	R1	85.037 ± 3.98	108.3 ± 2.731	--	0.737
					R2	0.367 ± 0.099	0.332 ± 0.049	--	
					R3	71.305 %	66.2%	--	
F2	2.0 g	3.934 ml	9.0 ml	3.737	R1	85.037 ± 1.87	119.2 ± 3.85	--	0.732
					R2	0.396 ± 0.055	0.485 ± 0.032	--	
					R3	75.161 %	76%	--	
F3	2.0 g	3.833 ml	8.997 ml	3.527	R1	85.035 ± 2.77	89.65 ± 1.721	0.151749518	0.729
					R2	0.402 ± 0.069	0.392 ± 0.002	0.421648255	
					R3	76.024 %	76.6%	0.364331832	

2.2. Characterization

2.2.1. Vesicle size and PDI

Tables 1 and 2 show the mean Vesicle size and PDI for the developed formulations. The LSP-PMs dispersions had vesicles with sizes ranging from 337.9 ± 15.933 to 85.0367 ± 1.304 nm and PDI varying from 0.26 ± 0.025 to 0.513 ± 0.011. Three optimized batches were made and validated as per the DOE prediction. The batch with the vesicle size 89.65 ± 1.721 nm with a polydispersity index of 0.392 ± 0.002 showing homogeneity (Difference is non-significant at $P>0.05$) was selected as the final optimized batch.

2.2.2. Calculation of encapsulation efficiency (%EE)

The volume of solvents and the drug's solubility in the lipid have a big impact on the EE. The average % EE for all the created formulations is shown in Tables 1 and 2. The % EE of the LSP-PMs dispersions ranged from 42% to 86.736%. Three optimized batches were created and validated according to the DOE projection, and the selected optimized batch's %EE was found to be 76.6%.

2.2.3. Zeta Potential (ZP)

The ZP of nanocarriers is a feature that determines their physical stability. ZP is connected to the nanoparticle's charge at the surface and reflects the extent of repulsion among them. In formulations with ZP varying from -30 to +30 mV, particle aggregation is less frequent [31,32]. The optimized LSP-PMs had zeta potential values of 0.0259 mV. Steric stabilisation, also known as steric hindrance, is the cause of the stability of nanosized phospholipid magnesome formulations, even when the zeta potential is close to zero. This result is caused by a dense coating of hydrophilic molecules present on the surface of the nanoparticles. The phospholipid bilayer that makes up the exterior of phospholipid magnesomes at the nanoscale aids in the stability of these nanoparticles. The phospholipids' hydrophilic "head" regions are facing outward, which repels the nanoparticles. The arrangement of the phospholipids on the surface efficiently prevents particles from flocculating or settling out of the dispersion even if the zeta potential may be close to zero [33]. Thus, indicating that the system was physically stable. Furthermore, because of the likelihood of electrostatic interactions with negatively charged mucin, the mucoadhesive capabilities of the nanoparticles are the most crucial property of these positive zeta potentials.

2.2.4. Determination of Surface Morphology by Transmission Electron Microscopy (TEM)

Figure 4 (A, B, C and D graph) shows TEM micrographs of optimized LSP-PMs formulation that was obtained at various angles and scales which had slightly spherical particles with decreased vesicle size and a bilayer lipid structure. The irregular shapes of PMs can be traced to several underlying causes. First off, they are influenced by their flexible and dynamic nature, which allows them to deform, change shape, and undergo processes like fusion and fission. These atypical forms can result from complex interactions between lipid bilayer cargo and interior elements, and the presence of nearby molecules, ions, and surfaces. Environmental factors like temperature, pH, and ion concentration can also affect magnesomes' shapes,

potentially indicating thermodynamically stable or metastable states. In the TEM picture, the mean vesicle size of the optimized LSP-PMs was found to be 53.31 nm. Nanoparticles having a VS of less than 100 to 200 nm are essential for improved absorption through the nasal membrane. Furthermore, smaller vesicle size with high entrapment effectiveness has superior drug release control and easily crosses the BBB [16].

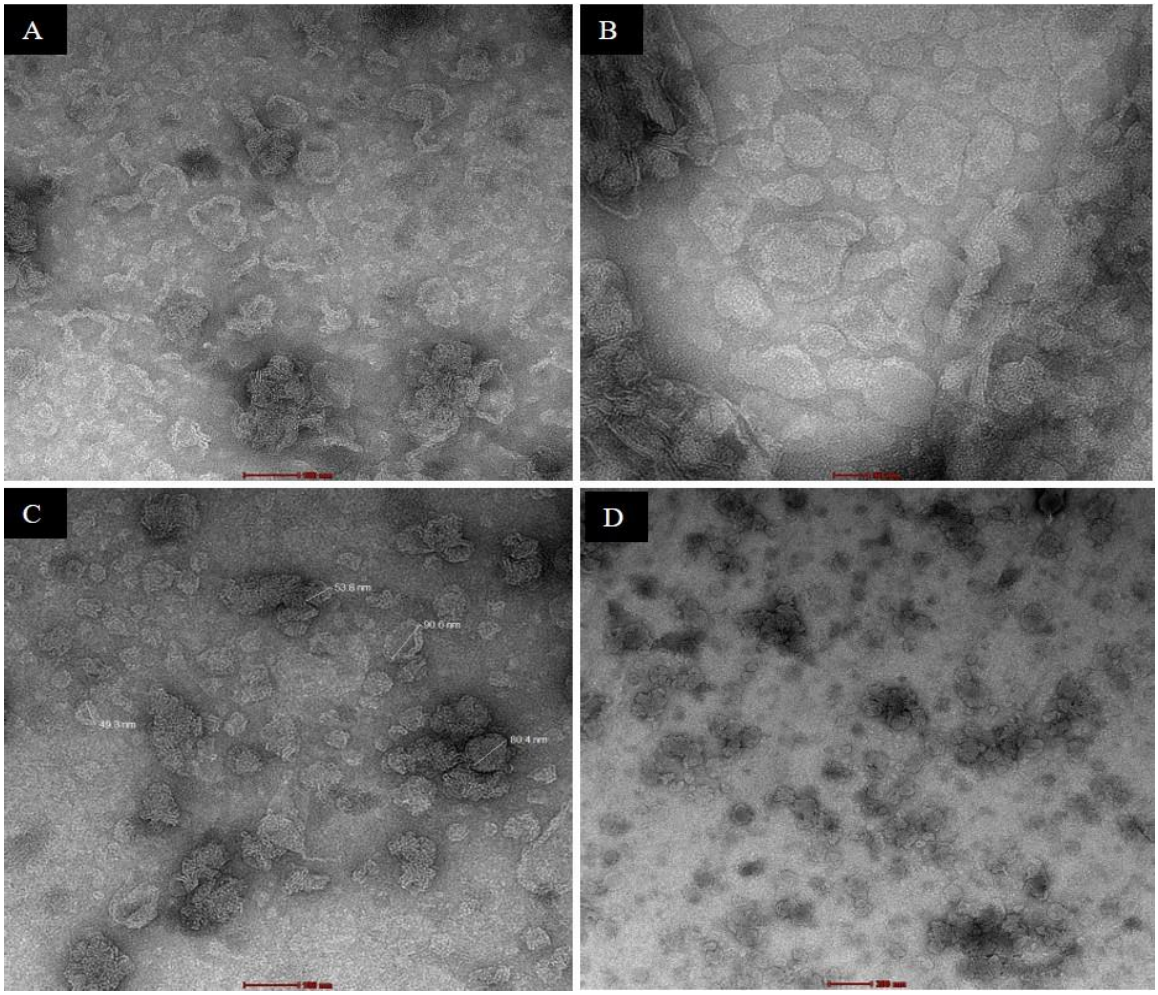

Figure 4. TEM images of optimized LSP-PMs

2.2.5. pH measurement and Viscosity measurement

To minimize nasal mucosa irritation and additional consequences on olfactory nerves and nasal ciliary, the pH of the nasal mucosa of humans shall be kept between the usual range of 5.5 to 6.5 [26]. The pH of the prepared optimized formulation was found to be 7.1 pH by which it was confirmed that the formulation was biocompatible.

Also, the viscosity of the prepared optimized formulation was found to be 3.297 ± 0.7 cP. A controlled and standardized environment is provided while doing viscosity studies at 25 °C. The behavior and stability of the nanosized phospholipid magnesomes are first understood by doing a viscosity investigation at 25 °C. Using this method enables us to collect the preliminary information prior to doing research at temperatures more similar to the environment of the nasal cavity [34].

2.2.6. Differential Scanning Calorimetry (DSC) study

The crystallinity of PMs must be characterized since it affects encapsulation and drug release [31]. DSC investigations were carried out to learn about the melting point %EE and crystallinity of the LSP and LSP-PMs optimized formulation. Figure 5 (a) shows the pure drug's DSC curve, which gives the endothermic peak between 190-200^{o}C, similar to the drug's melting point. While figure 5 (b) shows the DSC curve of the LSP-PMs optimized mixture, which did not indicate a thermal event at 190-200 ^{o}C that is attributable to LSP's melting point, indicating that the API is amorphous or is distributed adequately in the matrices of lipid.

2.2.7. Powder X-ray Diffraction (P-XRD) study

The P-XRD method was employed to evaluate the crystallinity of the LSP and LSP-PMs. The diffractograms of LSP and LSP-loaded PMs (optimized) are depicted in figure 6(A) and (B), respectively. LSP's major peaks in the figure illustrate the XRD patterns. The levosulpiride pattern revealed intrinsic peaks at 2θ distributed angles of 10.5, 11.1, 12.9, 14.6, 15.2, 16.9, 18, 19.8, 21.1, 22.1, 24, 24.6, 25.9, 29.7, and 30 defining regular crystalline structure. On the other hand, optimized LSP-loaded PMs show no particular levosulpiride peaks confirming the drug's change from crystalline to amorphous form into the matrix of lipids.

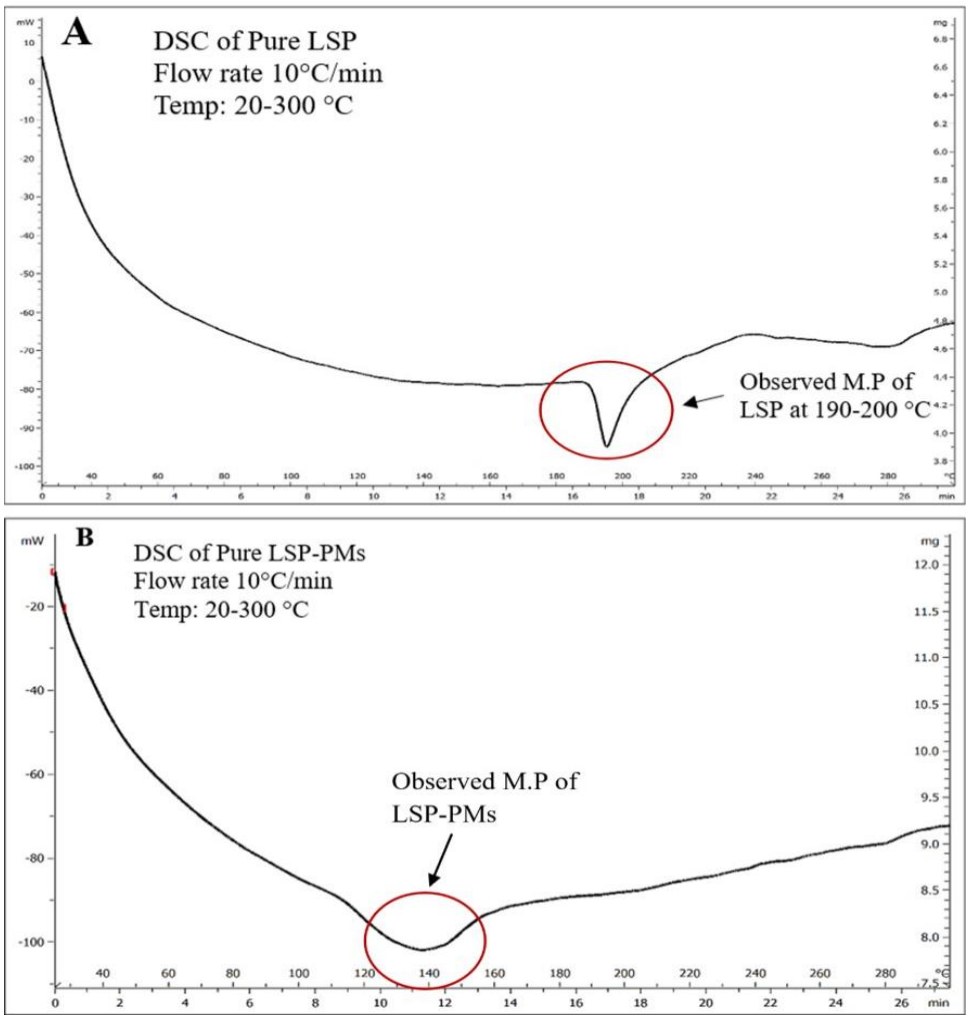

Figure 5A & 5B. DSC image of LSP & DSC image of LSP-PMs mixture respectively

2.2.8. Fourier-Transform Infrared Spectroscopy (FTIR)

In Figure 7A, which is LSP's FTIR graph, vibrations at 3370.35 cm-1, 3270.77 cm-1, and 3112.79 cm-1 reflect the N-H bond of an amide, a bond of sulfonamide, and an aromatic group, respectively. The existence of the C-H group of the methyl and methylene functional groups was demonstrated by the vibrations at 2968.00 cm-1 and 2873.57 cm-1. Peaks at 1621.10 cm -1 show amide group C=O stretching, while 1544.12 cm -1 represents C=C (aromatic) bending. The C-H (aromatic) and C-O (methoxy) group vibrations were shown by peaks at 1287.90 cm-1 and 834.16 cm-1, respectively. Moreover, the distinctive FTIR peaks of LSP were displaced in the FTIR spectra of optimized LSP-PMs, depicting that LSP was successfully incorporated into the lipid core (Figure 7B).

The chemical stability of the medication and its change from crystalline to amorphous form is demonstrated by XRD analysis and FTIR data, respectively. These findings also show that PMs can improve LSP's bioavailability by enhancing solubility due to phase transition. The dissolution profile of LSP-PMs was

studied to confirm the findings.

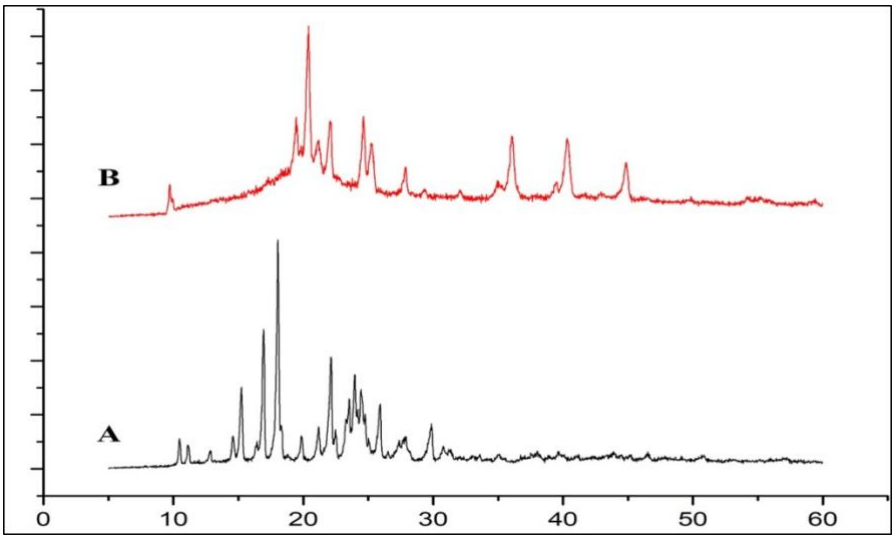

Figure 6 (A) and (B). XRD graphs of LSP and LSP-PMs, respectively

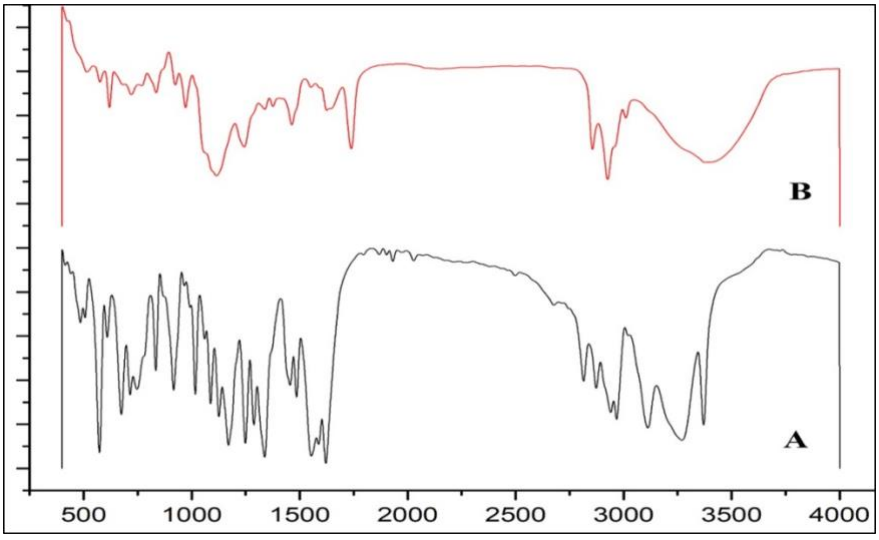

Figure 7(A) and (B). FTIR graphs of LSP and LSP-PMs, respectively

2.2.9. Invitro drug release study

The findings of *invitro* release tests using optimized batch of LSP-PMs and suspension of LSP are given in Figure 8. In order to achieve accurate measurements of dissolution rates and to reduce any potential impacts of saturation on the outcomes, sink conditions were maintained. In the LSP-PMs optimized formulation, the fastest drug release was within an hour which was constantly increasing. While in the API suspension, the release was initially low, then raised after 2 hours, and the 100% release was at 3.5 hours. From the results, it can be said that the optimized LSP-PMs formulation gives the fastest drug release, which was 3.5 folds faster as compared to the LSP-suspension.

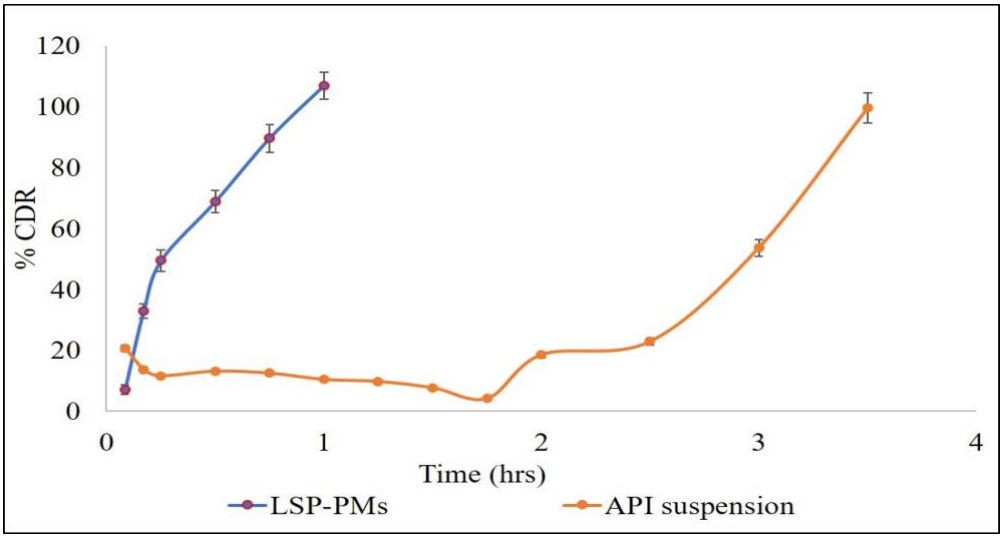

Figure 8. Drug diffusion of optimized LSP-PMs and LSP-solution

2.2.10. Stability study

The accelerated stability study was employed in accordance with ICH Q1A (R2) guidelines. Here the batch was stored at ambient temperature (either 25°C ± 2°C/60% RH ± 5% RH or 30°C ± 2°C/65% RH ± 5% RH) for 50 days, and the evaluation was carried out for Vesicle size, PDI, and %EE after every 10 days till 50 days. The selected temperature and humidity levels were purposefully chosen to simulate real-world environmental conditions that the products may encounter during storage and distribution. The humidity and temperature sensors were kept with the formulation to check the temperature and humitity level throughout the study. The stability data showed (Table 3) that the LSP-PMs formulation was stable at ambient temperature for 50 days with no notable change in Vesicle size, PDI, and EE (%). Table 3 shows the stability data of the optimized LSP-PMs batch.

Table 3. Stability data of LSP-PMs formulation.

Days	Vesicle Size	PDI	%EE
0	89.65 ± 2.517	0.392 ± 0.084	76.6
10	99.06 ± 5.84	0.316 ± 0.003	76.1
20	105.05 ± 1.114	0.377 ± 0.054	77.3
30	108.363 ± 4.62	0.38 ± 0.0215	73.5
40	110.9 ± 3.489	0.41 ± 0.077	73.72
50	109.87 ± 1.58	0.36 ± 0.025	74.2

3. CONCLUSION

In this study, we aimed to create Levosulpiride-loaded Phospholipid Magnesomes (PMs), a novel vesicular nanosystem that was recently created for brain targeting, prepared of phospholipon 90G, ethanol, propylene glycol, magnesium sulphate, and water with the goal of providing targeted administration of Levosulpiride, directly to the brain via olfactory route while also optimizing it, and counteracting the P-gp efflux effect. Design expert® version-13 and BBD were employed with 29 runs for the optimization of the formulation. Using the amount of phospholipid, ethanol, and propylene glycol, as well as the sonication time as independent variables, the LSP-PMs systems were optimized for higher %EE, smaller vesicle size, and PDI. From the DoE results, the LSP-PMs dispersions had vesicles with sizes ≤ 400 nm, and PdI exhibited consistent variation, consistently measuring ≤ 0.55. The %EE also varied constantly, consistently ≥ 40%. Three optimized batches were made and validated as per the DOE prediction, and the optimized LSP-PMs formula had a vesicle size of 85.035 ± 2.77 nm, a PDI of 0.392 ± 0.69, and an %EE of 76.024 %. DSC, FTIR, and XRD solid-state characterization experiments revealed amorphous drug dispersion within the lipid matrix

and high compatibility between LSP and formulation constituents. The optimized LSP-PMs formula had the fastest drug-releasing profile, reaching 100% in 1 hour. Stability was carried out for 50 days, where after every 10 days, evaluation of Vesicle size, PDI, and %EE was done. Stability data depicted that the formulation of LSP-PMs was stable at room temperature till 50 days. Thus, in this study, the nanovesicular system, i.e., LSP-PMs, was shown to be a potential formulation for improving drug release of weakly water soluble and permeable drug LSP while simultaneously providing a stable formulation when opposed to oral solution form. More research is needed to assess nasal transport to the brain, pharmacokinetic and pharmacodynamic effects, local safety, and the behavior of this carrier.

4. MATERIALS AND METHODS

4.1. Materials

The LSP was gifted by Prayosha Healthcare Pvt. Ltd. located in Gujarat, India. Lipoid (United States) provided a free sample of Phospholipon 90G (PL). LOBA Chemie Pvt. Ltd. (India) supplied Propylene Glycol (PG), Ethanol (AR grade), and Methanol (AR grade). Magnesium sulphate was purchased from Suvidhinath laboratories, Vadodara, India. Double distilled water was utilized throughout the research work. All other chemicals used were of analytical grade, they were in pure form, and were procured from common commercial suppliers.

4.2. Methodology

4.2.1. Box-Behnken Design (BBD) for optimization

The responses were evaluated using a statistical model that included interactive and polynomial factors. In this study, Design expert® 13th version was employed. With four components and three levels, the BBD was chosen to optimize the formulation variables for fabricating Levosulpiride PMs. The BBD is a nonlinear 2nd-order quadratic model, and when the factors are <6, BBD is utilized [35,36]. It has various advantages, such as requiring fewer experimental runs than CCD, obtaining a nonlinear effect, and being able to be used for product and process improvement[37,38].

The amount of Phospholipon 90G as a phospholipid (A), amount of Ethanol (B), amount of propylene glycol (C), and time of sonication (D) were chosen as independent factors. Every factor was assigned a high, middle, and low level. The vesicle size (VS), PDI, and extent of encapsulation (%EE) were taken as dependent variables. Tables 4 and 5 provide background information about the design and the values assigned to the design, respectively. Table 6 depicts the actual amount of chemicals taken in accordance with the design.

Table 4. Short description of the design

Sr. no	Design	Criteria
1	Independent variables	Amount of Phospholipon 90G (mg or g) Amount of Ethanol (ml) Amount of propylene glycol (ml) Sonication time (min)
2	Number of runs	29

4.2.2. Method of Preparation

The ultrasonication approach was used to prepare LSP-PMs using a probe sonicator. To begin, the phospholipid, i.e., phospholipon 90G, was broken down in a solution of propylene glycol and ethanol. LSP was incorporated into the lipid phase after full dissolution. Simultaneously, an aqueous solution containing 0.02mg of magnesium sulphate ($MgSO_4$) was prepared and introduced to the lipid phase in drops using a 1ml syringe. Before sonication, the mixture was briefly mixed on a magnetic stirrer at 700 rpm. A probe

sonicator was used for further sonication. As preliminary trial batches, placebos of PMs having no medication (blanks) were also created [20,22].

Table 5. Assignment of values in design and independent and dependent variables and levels.

Independent variables	Levels		
	Low	Intermediate	High
Coded values	**-1**	**0**	**+1**
A-Amount of phospholipon 90G (gm)	1	1.5	2
B-Amount of ethanol (ml)	1	3	5
C-Amount of propylene glycol (ml)	9	6	9
D-Sonication time (min)	3	9	15
Dependent variables	Vesicle size, PDI, and Drug Entrapment		

4.3. Characterization

4.3.1. Vesicle size and PDI

Dynamic light scattering (DLS) on a Malvern Zetasizer was utilized for measuring the average Vesicle size and PDI. Both blank and LSP-PMs were analyzed. For each formulation, three replicate analyses were done, and findings were given as mean ± SD [39–42].

4.3.2. Calculation of encapsulation efficiency (%EE)

Drug encapsulation efficiency (%EE) refers to the amount (%) of API encapsulated by the PMs.The dialysis technique was employed to calculate the EE (%). In the dialysis bag, 1 ml of the formulation was introduced. The dialysis bag was kept in 200ml of water and spun in a rotary shaker for 2 hours. Following 2 hours, the sample was taken out from the bag and diluted with methanol to a volume of 10ml. The free drug was then calculated employing a UV-Visible Spectroscopy at 289 nm. The formula given below was utilized to compute the EE (%)[41,43]:

EE (%) = (Drug Obtained) / (Total drug) × 100

4.3.3. Zeta Potential (ZP)

The ZP is a characteristic that determines the nanocarrier's stability (physical). It is connected to nanoparticle surface charge and reflects the repulsion among them. The ZP of the LSP-PMs was measured utilizing the Zetasizer Nano ZS90. Small-volume disposable zeta cells were used for measurements [32,39,41].

Table 6. Actual amount and preparation of batches according to the design

Batch no:	Factor 1	Factor 2	Factor 3	Factor 4
	A: Amount of PL 90G	B: Amount of Ethanol	C: Amount of PG	D: Sonication Time
	gm	ml	ml	Min
1	1.5	1	6	15
2	1.5	3	6	9
3	1	3	6	15
4	2	5	6	9
5	1.5	3	3	3
6	1.5	3	3	15
7	1.5	3	6	9
8	1.5	3	6	9
9	1	3	9	9
10	1.5	1	9	9
11	2	3	6	3
12	1.5	3	6	9
13	2	3	6	15
14	1	1	6	9
15	1	5	6	9
16	1.5	5	6	15
17	2	3	3	9
18	2	1	6	9
19	1.5	5	9	9
20	1.5	1	3	9
21	1.5	5	3	9
22	1.5	3	9	3
23	1.5	1	6	3
24	1.5	3	6	9
25	1	3	3	9
26	1.5	3	9	15
27	1.5	5	6	3
28	2	3	9	9
29	1	3	6	3

4.3.4. Determination of Surface Morphology by Transmission Electron Microscopy (TEM)

A TEM (JEOL, Japan) was employed to determine the surface characteristics of LSP-PMs. Using a glass capillary, a small amount of formulation was added on a grid made of copper (300#), which was coated with carbon. The formulation-loaded copper grid was then dried in air at ambient temperature for 4 hours. After drying, the copper grid was kept in an ion cleaner for two minutes. The material was

photographed using a transmission electron microscope [42].

4.3.5. pH and Viscosity measurement

The pH of the optimized formula is a critical criterion to ensure that it is not associated with the inflammation of nasal tissue [11]. The pH of the LSP-PMs batch was evaluated employing a pH meter. RhealabQC (Anton Paar) and DG 26.7 at 25^{o} C were used for viscosity measurement.

4.3.6. Differential Scanning Calorimetry (DSC) study

To investigate the heat stability and compatibility of excipients, DSC research (TGA-DSC-1 METTLER TOLEDO) was performed on pure excipients and mixtures of LSP and excipients. By correctly mixing LSP and excipients, a mixture of LSP and excipients was prepared. As a reference, an empty crucible was used. LSP was then precisely weighed and deposited in the crucible. The analysis was performed in an environment containing nitrogen at a rate of scanning: 10°C/min in a temperature ranging from 20°C-300°C [41].

4.3.7. Powder X-ray Diffraction (P-XRD) study

The crystalline nature of LSP is determined by P-XRD (Bruker D-2 phaser). The PMs dispersions (unloaded PMs and LSP-PMs) were cryoprotected by freeze-drying with mannitol. The diffraction patterns of the LSP-PMs and pure LSP were obtained employing a Powder X-ray Diffractometer (D2-phaser, Bruker) under the following conditions: ambient temperature, Cu Kα radiations generated at 40 kV voltage and 20 mA, and steps of 0.02^{o} for 2s with a scanning speed of 0.03^{o}s^{-1} in the intermission 2θ at 10-60°C [41].

4.3.8. Fourier-Transform Infrared Spectroscopy (FTIR)

The FTIR method was employed to measure the encapsulation of medicine within PMs [16]. To investigate this, FTIR spectroscopy was used on pure LSP and LSP-PMs formulation. These samples were dispersed with KBr, and a pellet was formed. Prepared pellets were scanned in the range of 4000cm^{-1} - 500cm^{-1} [41,42].

4.3.9. Release of the drug: In vitro study

The Diffusion technique was utilized to measure the *in vitro* drug release patterns of optimized formulation of nanoparticles. In a 25 ml Franz diffusion cell, the reservoir chamber was loaded with 25 ml phosphate buffer solution (PBS), whose pH was 6.4. Upon that, an activated dialysis membrane was kept, and in the donor compartment, 1ml of PMs formulation was filled. The dialysis membrane utilized was of 12000-14000 DA with 2.4nm pore size. One ml of buffer solution is removed at 5,10, 15 minutes, and every 15 minutes for 2 hours, then at an hour interval for 24 hours, and promptly replaced by an equal volume of PBS pH6.4. UV visible spectroscopy is used to detect the drug concentration at 292nm [32,42,44].

4.3.10. Stability study (SS)

The accelerated SS was conducted in accordance with ICH Q1A (R2) guidelines. The drug-loaded PMs formulation was kept at room temperature for 50 days (either 25°C ± 2°C/60% RH ± 5% RH or 30°C ± 2°C/65% RH ± 5% RH). The sensors were kept with the formulation the measure the temperature and humidity level throughout the study. The SS of the Optimized batch of LSP-PMs was performed at the intervals of 10 days till 50 days of storage; the following characterization was carried out: Vesicle size, PDI, and %EE [45].

Acknowledgements: The authors are thankful to Ramanbhai Patel College of Pharmacy, Charotar University of Science and Technology, for extending their facility to carry out work.

Author contributions: Concept – R.J.P., N.T.; Design – R.J.P., N.T.; Supervision – R.J.P.; Resources – V.P., A.A.P.; Materials – A.A.P.; Data Collection and/or Processing – R.J.P., N.T., V.P.; Analysis and/or Interpretation – R.J.P., N.T., S.G.P.; Literature Search – N.T.; Writing – N.T., V.P.; Critical Reviews – R.J.P., N.T., V.P., A.A.P., S.G.P., B.G.P.

Conflict of interest statement: The authors declared no conflict of interest.

Declarations: This article does not contain any studies with human participants or animals performed by any author.

8. REFERENCES

[1] Insel TR. Rethinking schizophrenia. Nature. 2010;468(7321):187–193. https://doi.org/10.1038/nature09552
[2] Kahn RS, Sommer IE, Murray RM, Meyer-Lindenberg A, Weinberger DR, Cannon TD, O'Donovan M, Correll CU, Kane JM, van Os J, Insel TR. Schizophrenia. Nat Rev Dis Primers. 2015;1:15067. https://doi.org/10.1038/nrdp.2015.67 .
[3] McCutcheon RA, Reis Marques T, Howes OD. Schizophrenia-An Overview. JAMA Psychiatry.2020;77(2):201-210. https://doi.org/10.1001/jamapsychiatry.2019.3360
[4] Correll CU. Current Treatment Options and Emerging Agents for Schizophrenia. J Clin Psychiatry. 2020;81(3):MS19053BR3C. https://doi.org/10.4088/jcp.ms19053br3c .
[5] Rossi F, Forgione A. Pharmacotoxicological aspects of levosulpiride. Pharmacol Res . 1995;31(2):81–94. https://doi.org/10.1016/1043-6618(95)80052-2
[6] Poorani G, Uppuluri S, Uppuluri KB. Formulation, characterization, in vitro and in vivo evaluation of castor oil based self-nano emulsifying levosulpiride delivery systems. J Microencapsul. 2016;33(6):535–543. http://dx.doi.org/10.1080/02652048.2016.1223199
[7] Chitneni M, Peh KK, Darwis Y, Abdulkarim M, Abdullah GZ, Qureshi MJ. Intestinal permeability studies of sulpiride incorporated into self-microemulsifying drug delivery system (SMEDDS). Pak J Pharm Sci. 2011;24(2):113–121.
[8] Kim DS, Kim DW, Kim KS, Choi JS, Seo YG, Youn YS, Oh KT, Yong CS, Kim JO, Jin SG, Choi HG. Development of a novel l-sulpiride-loaded quaternary microcapsule: Effect of TPGS as an absorption enhancer on physicochemical characterization and oral bioavailability. Colloids Surf B Biointerfaces. 2016;147:250-257. http://dx.doi.org/10.1016/j.colsurfb.2016.08.010
[9] Ibrahim WM, AlOmrani AH, Yassin AEB. Novel sulpiride-loaded solid lipid nanoparticles with enhanced intestinal permeability. Int J Nanomed. 2013;9(1):129–144. http://dx.doi.org/10.2147/IJN.S54413
[10] Khaleeq N, Din FU, Khan AS, Rabia S, Dar J, Khan GM. Development of levosulpiride-loaded solid lipid nanoparticles and their in vitro and in vivo comparison with commercial product. J Microencapsul. 2020;37(2):160–169. http://dx.doi.org/10.1080/02652048.2020.1713242
[11] Salem LH, El-Feky GS, Fahmy RH, El Gazayerly ON, Abdelbary A. Coated lipidic nanoparticles as a new strategy for enhancing nose-to-brain delivery of a hydrophilic drug molecule. J Pharm Sci. 2020;109(7):2237–2251. https://doi.org/10.1016/j.xphs.2020.04.007
[12] Agrawal M, Saraf S, Saraf S, Antimisiaris SG, Chougule MB, Shoyele SA, Alexander A. Nose-to-brain drug delivery: An update on clinical challenges and progress towards approval of anti-Alzheimer drugs. J Control Release. 2018;281:139-177. https://doi.org/10.1016/j.jconrel.2018.05.011
[13] Van Sorge NM, Doran KS. Dynamic epidemiology of bacterial meningitis. Futur Microbiol. 2012;7:383–394.
[14] Chauhan I, Yasir M, Verma M, Singh AP. Nanostructured lipid carriers: A groundbreaking approach for transdermal drug delivery. Adv Pharm Bull. 2020;10(2):150–165. https://doi.org/10.34172/apb.2020.021
[15] Patel AA, Patel RJ, Patel SR. Nanomedicine for intranasal delivery to improve brain uptake. Curr Drug Deliv. 2014;15:461-469. https://doi.org/10.2174/1567201814666171013150534
[16] Agbo CP, Ugwuanyi TC, Ugwuoke WI, McConville C, Attama AA, Ofokansi KC. Intranasal artesunate-loaded nanostructured lipid carriers: A convenient alternative to parenteral formulations for the treatment of severe and cerebral malaria. J Control Release. 2021;334:224–236. https://doi.org/10.1016/j.jconrel.2021.04.020
[17] van Woensel M, Wauthoz N, Rosière R, Amighi K, Mathieu V, Lefranc F, van Gool SW, de Vleeschouwer S. Formulations for Intranasal Delivery of Pharmacological Agents to Combat Brain Disease: A New Opportunity to Tackle GBM? Cancers (Basel). 2013;5(3):1020-1048. https://doi.org/10.3390%2Fcancers5031020 .
[18] Costantino HR, Illum L, Brandt G, Johnson PH, Quay SC. Intranasal delivery: Physicochemical and therapeutic aspects. Int J Pharm. 2007;337(1–2):1–24. https://doi.org/10.1016/j.ijpharm.2007.03.025
[19] Agrawal M, Saraf S, Saraf S, Dubey SK, Puri A, Patel RJ, Ajazuddin, Ravichandiran V, Murty US, Alexander A. Recent strategies and advances in the fabrication of nano lipid carriers and their application towards brain targeting. J Control Release. 2020;321:372-415. https://doi.org/10.1016/j.jconrel.2020.02.020
[20] Natsheh H, Touitou E. Phospholipid magnesome—A nasal vesicular carrier for delivery of drugs to brain. Drug Deliv Transl Res. 2018;8(3):806–819. https://doi.org/10.1007/s13346-018-0503-y
[21] Touitou E, Duchi S, Natsheh H. A new nanovesicular system for nasal drug administration. Int J Pharm. 2020;580:119243. https://doi.org/10.1016/j.ijpharm.2020.119243
[22] Sayyed ME, El-Motaleb MA, Ibrahim IT, Rashed HM, El-Nabarawi MA, Ahmed MA. Preparation, characterization, and in vivo biodistribution study of intranasal 131I-clonazepam-loaded phospholipid magnesome as a promising brain delivery system: Biodistribution and pharmacokinetic behavior of intranasal 131I-Clonazepam loaded phospholip. Eur J Pharm Sci. 2022;169:106089. https://doi.org/10.1016/j.ejps.2021.106089
[23] Verma P, Pathak K. Nanosized ethanolic vesicles loaded with econazole nitrate for the treatment of deep fungal infections through topical gel formulation. Nanomed Nanotechnol Biol Med. 2012;8(4):489–496. http://dx.doi.org/10.1016/j.nano.2011.07.004
[24] Dubey V, Mishra D, Jain NK. Melatonin loaded ethanolic liposomes: Physicochemical characterization and enhanced transdermal delivery. Eur J Pharm Biopharm. 2007;67(2):398–405. https://doi.org/10.1016/j.ejpb.2007.03.007
[25] Christensen R. Analysis of Variance, Design, and Regression. Linear Modeling for Unbalanced Data, Second Edition. Chapman and Hall/CRC, New York, 2016. http://dx.doi.org/10.1201/9781315370095

[26] Abourehab MAS, Khames A, Genedy S, Mostafa S, Khaleel MA, Omar MM, El Sisi AM. Sesame Oil-Based Nanostructured Lipid Carriers of Nicergoline, Intranasal Delivery System for Brain Targeting of Synergistic Cerebrovascular Protection. Pharmaceutics. 2021;13(4):581. https://doi.org/10.3390/pharmaceutics13040581
[27] Khames A. Preparation and characterization of sildenafil loaded solid lipid nanoparticles: Drug delivery system suitable for nebulization. Sch Res Libr. 2017;9(3):98–112. http://scholarsresearchlibrary.com/archive.html
[28] Khames A, Khaleel MA, El-Badawy MF, El-Nezhawy AOH. Natamycin solid lipid nanoparticles - sustained ocular delivery system of higher corneal penetration against deep fungal keratitis: Preparation and optimization. Int J Nanomed. 2019;14:2515–2531. http://dx.doi.org/10.2147/IJN.S190502
[29] Nasr A, Gardouh A, Ghonaim H, Abdelghany E, Ghorab M. Effect of oils, surfactants and cosurfactants on phase behavior and physicochemical properties of self-nanoemulsifying drug delivery system (SNEDDS) for irbesartan and olmesartan. Int J Appl Pharm. 2016;8(1):13–24. https://doi.org/10.22159/ijap.2016v8i1.10530
[30] Khames A. Formulation and characterization of eplerenone nanoemulsion liquisolids, an oral delivery system with higher release rate and improved bioavailability. Pharmaceutics. 2019;11(1):40. https://doi.org/10.3390/pharmaceutics11010040
[31] Matarazzo AP, Elisei LMS, Carvalho FC, Bonfílio R, Ruela ALM, Galdino G, Pereira GR. Mucoadhesive nanostructured lipid carriers as a cannabidiol nasal delivery system for the treatment of neuropathic pain. Eur J Pharm Sci. 2021;159:105698. https://doi.org/10.1016/j.ejps.2020.105698
[32] Müller RH, Mäder KSG. Solid lipid nanoparticles (SLN) for controlled drug delivery - a review of the state of the art. Eur J Pharm Biopharm. 2000;50(1):161–177. https://doi.org/10.1016/S0939-6411(00)00087-4
[33] Minnelli C, Moretti P, Fulgenzi G, Mariani P, Laudadio E, Armeni T, Galeazzi R, Mobbili G. A Poloxamer-407 modified liposome encapsulating epigallocatechin-3-gallate in the presence of magnesium: Characterization and protective effect against oxidative damage. Int J Pharm. 2018;552(1-2):225-234. https://doi.org/10.1016/j.ijpharm.2018.10.004
[34] El-Housiny S, Shams Eldeen MA, El-Attar YA, Salem HA, Attia D, Bendas ER, El-Nabarawi MA. Fluconazole-loaded solid lipid nanoparticles topical gel for treatment of pityriasis versicolor: formulation and clinical study. Drug Deliv. 2018 Nov;25(1):78-90. doi: 10.1080/10717544.2017.1413444. Erratum in: Drug Deliv. 2018 Nov;25(1):2015. https://doi.org/10.1080/10717544.2017.1413444 .
[35] Ferreira SL, Bruns RE, Ferreira HS, Matos GD, David JM, Brandão GC, da Silva EG, Portugal LA, dos Reis PS, Souza AS, dos Santos WN. Box-Behnken design: an alternative for the optimization of analytical methods. Anal Chim Acta. 2007;597(2):179-186. http://doi.org/10.1016/j.aca.2007.07.011
[36] Karmoker JR, Hasan I, Ahmed N, Saifuddin M, Reza MS. Development and Optimization of Acyclovir Loaded Mucoadhesive Microspheres by Box – Behnken Design. Dhaka Univ J Pharm Sci. 2019;18(1):1–12. http://doi.org/10.3329/dujps.v18i1.41421
[37] Hao J, Fang X, Zhou Y, Wang J, Guo F, Li F, Peng X. Development and optimization of solid lipid nanoparticle formulation for ophthalmic delivery of chloramphenicol using a Box-Behnken design. Int J Nanomedicine. 2011;6:683-692. http://dx.doi.org10.2147/ijn.s17386
[38] Pramod K, Tahir Ma, Charoo N, Ansari S, Ali J. Pharmaceutical product development: A quality by design approach. Int J Pharm Investig. 2016;6(3):129–138. http://doi.org/10.4103/2230-973X.187350
[39] Cunha S, Forbes B, Lobo JMS, Silva AC. Improving drug delivery for alzheimer's disease through nose-to-brain delivery using nanoemulsions, nanostructured lipid carriers (NLC) and in situ hydrogels. Int J Nanomed. 2021;16:4373–4390. https://doi.org/10.2147/IJN.S305851
[40] Alam MI, Baboota S, Ahuja A, Ali M, Ali J, Sahni JK. Intranasal administration of nanostructured lipid carriers containing CNS acting drug: Pharmacodynamic studies and estimation in blood and brain. J Psychiatr Res. 2012;46(9):1133–1138. http://dx.doi.org/10.1016/j.jpsychires.2012.05.014
[41] Patel RJ, Patel ZP. Formulation optimization and evaluation of nanostructured lipid carriers containing valsartan. Int J Pharm Sci Nanotechnol. 2013;6(2):2077–2086. http://doi.org/10.37285/ijpsn.2013.6.2.10
[42] Rathod K, Ahmed H, Gomte SS, Chougule S, A P, Dethe MR, Patel RJ, Bharadwaj D, Alexander A. Exploring the potential of anti-inflammatory activity of berberine chloride-loaded mesoporous silica nanoparticles in carrageenan-induced rat paw edema model. J Solid State Chem. 2023;317(Part A):123639. https://doi.org/10.1016/j.jssc.2022.123639
[43] Eskandari S, Varshosaz J, Minaiyan M, Tabbakhian M. Brain delivery of valproic acid via intranasal administration of nanostructured lipid carriers: in vivo pharmacodynamic studies using rat electroshock model. Int J Nanomed. 2011;6:363–371. https://doi.org/10.2147/IJN.S15881
[44] Costa CP, Moreira JN, Sousa Lobo JM, Silva AC. Intranasal delivery of nanostructured lipid carriers, solid lipid nanoparticles and nanoemulsions: A current overview of in vivo studies. Acta Pharm Sin B. 2021;11(4):925–940. https://doi.org/10.1016/j.apsb.2021.02.012
[45] Agrawal M, Saraf S, Pradhan M, Patel RJ, Singhvi G, Ajazuddin, et al. Design and optimization of curcumin loaded nano lipid carrier system using Box-Behnken design. Biomed Pharmacother. 2021;141(May):111919. https://doi.org/10.1016/j.biopha.2021.111919